



## Full Length Article

## Effects of particle size on the self-ignition behaviour of a coal dust layer on a hot plate

Bei Li<sup>a,b</sup>, Mengjia Li<sup>a</sup>, Wei Gao<sup>a</sup>, Mingshu Bi<sup>a</sup>, Li Ma<sup>b</sup>, Qihua Qin<sup>a</sup>, Chi-Min Shu<sup>c,\*</sup><sup>a</sup> School of Chemical Engineering, Dalian University of Technology, Dalian, Liaoning 116024, PR China<sup>b</sup> Key Laboratory of Western Mine Exploitation and Hazard Prevention, Xi'an University of Science and Technology, Xi'an, Shaanxi 710054, PR China<sup>c</sup> Department of Safety, Health, and Environmental Engineering, National Yunlin University of Science and Technology, Douliu, Yunlin 64002, Taiwan, ROC

## ARTICLE INFO

## Keywords:

Coal particle  
 Ignition behavior  
 Particle size  
 Minimum ignition temperature  
 Ignition delay time

## ABSTRACT

Knowing the sizes of coal particles is vital for understanding the real ignition behaviour of coal dust deposits on a hot plate. Furthermore, such knowledge facilitates model construction for assessing industrial coal dust explosion risk. Three particle sizes (0.10–0.15, 0.15–0.20, and 0.20–0.30 mm) of coal samples were selected to analyse the influence of particle size on ignition and smouldering behaviour. Characteristic parameters, such as the minimum ignition temperature of a dust layer (MITL), highest temperature in a layer (HTL), ignition delay time, and heating rates were tested and analysed using a dust layer ignition apparatus. The results revealed that the MITL was 200–210 °C and that the MITL tended to decrease with particle size. The aggregation effect improved the MITL containing fine particles. The optimal ignition position was 7.2 mm from the hot plate. As the particle size increased, the ignition delay time of the sample became longer. However, the HTL and the time to reach the maximum temperature reduced accordingly. For corresponding geometrical shapes of a coal dust layer, the results demonstrated that particle size had a limited effect on the void fraction but had a considerable effect on the number of particles. The finer coal dust had a substantial number of particles, thus producing a larger overall specific surface area in which to oxidize and devolatilize. Small coal dust particles pose a severe hazard in industrial sites, and thus, sites should be cleaned regularly to avoid the possibility of unwanted fires or explosions.

## 1. Introduction

Accidental coal dust explosions and fires are considered major impediments to the productive use of coal. However, the upside of the high combustibility of coal dust is that it is now the subject of research more than in the past, and thus, new applications for it are being found [1,2]. The massive amount of coal dust present at industrial sites, such as power plants and chemical plants, means that self-ignition or spontaneous combustion hazards exist in many places, from processing areas to final fuel preparation sites [3,4]. The layers of coal dust deposited on hot surfaces of equipment and within facilities can lead to instant ignition. Thus, fires or explosions may occur, especially when the ambient temperature is high. Such accidents cause substantial losses in terms of personnel and property and have a considerably negative social effect [5]. An example of such an accident is the large-scale pulverised coal dust explosion at the Hengda coal mine in 2014 (a subsidiary of Liaoning Fuxin Mining Ltd., Liaoning Province, China) that caused 26 fatalities.

In practice, coal dust at the coalface is mainly caused by the crushing and throwing involved in heavily mechanised coal exploitation. The particle size of the mine's coal dust was determined by screening the dust with a US standard 20-mesh sieve (850 µm) [6]. Moreover, 20% of the dust passed through a 200-mesh sieve (74 µm). Sapko et al. reported that approximately 60–77% (± 14) of the dust had a particle size less than 212 µm. Other reports [7] also verified that the particle sizes of coal dust at the working face were in the range of 1–200 µm, with a median particle size ( $d_{50}$ ) of 98.47 µm. According to the size of the particulate matter, the dustfall of pulverised coal comprised particles with a size larger than 100 µm that precipitated fastest due to the action of gravity. All suspended particles were solid particles with a particle size in the range of 10–100 µm. Moreover, the inhalable particulate matter had a particle size less than 10 µm. All these types of coal dust were present in the coal-related industrial premises, where fire and explosion hazards are numerous. Many scholars have investigated the ignition and smouldering characteristics of dust layers [8–12]. Among them, Hertzberg et al. explored the influence of the

\* Corresponding author.

E-mail address: [shucm@yuntech.edu.tw](mailto:shucm@yuntech.edu.tw) (C.-M. Shu).

**Nomenclature**

$A$	Particle cross section, $\text{mm}^2$
$A_c$	Base area of the ring, $\text{mm}^2$
$d$	Diameter of a single coal particle, mm
$d_{50}$	Median particle size, $\mu\text{m}$
$h$	Height of the control volume of the coal layer, mm
$H$	Height of the metal ring, mm
$N_l$	Number of particles in various directions
$N_b$	Number of coal particles
$t_{id}$	Ignition delay time, min
$t_{max}$	Time at which maximum temperature reached, min
$V_b$	Volume of the coal, $\text{mm}^3$
$V_c$	Control volume of the coal layer, $\text{mm}^3$
$V_{bs}$	Volume of a single coal particle, $\text{mm}^3$
MITL	Minimum ignition temperature of the layer, $^{\circ}\text{C}$

OIP	Optimal ignition position
HTL	Highest temperatures in the layer, $^{\circ}\text{C}$
PSD	Particle size distribution
SEM	Scanning electron microscope

*Greek symbols*

$\varepsilon$	Void fraction of coal powder layer, %
---------------	---------------------------------------

*Subscripts*

ad	Air-dried basis
daf	Dry ash-free basis
$x$	X direction
$y$	Y direction
$z$	Z direction

particle sizes of bituminous coal and polyethylene on lean flammability and thermal ignitability [9]. The authors found that the lean limit of flammability and the minimum ignition temperature of a layer (MITL) increased as the dust particle size increased. Furthermore, Zhang *et al.* studied the effects of particle size on ignition, combustion stability, and burnout properties. They showed that combustion characteristics were affected by particle size because of variations in specific surface area and pore structure [10]. Polka *et al.* measured the smouldering characteristic parameters of pulverised coal layers by using a hot plate [11]. Yuan *et al.* indicated that the MITL and ignition delay time of magnesium powder on a hot plate decreased as dust layer thickness increased, where the MITL increased from 710 to 760 K as the particle size increased from 6 to 173  $\mu\text{m}$  [12]. Garcia-Torrenta *et al.* used a Dengwen oven to test the MITL of six coal and biomass materials to evaluate inherent self-ignition hazards [13]. In conclusion, the ignition characteristics pertaining to material type, pore structure, ignition time, and dust layer thickness have been explored intensively by other researchers [10–12]. The size of coal particles in a thermodynamic state space is a crucial factor that affects real smouldering combustion behaviour and thus is a primary factor in the assessment of fire and explosion hazards [6,10]. However, the self-ignition behaviours of pulverised coal deposits with different particle sizes based on the thermodynamic geometry state have not been adequately studied. The

mechanism by which particle size influences the ignition characteristics of coal dust layers still requires further investigation. As a preventive measure, the temperature of hot surfaces must be regulated and maintained at a temperature below that at which ignition becomes possible. Therefore, research on the ignition and smouldering characteristics of coal dust layers with different particles sizes on hot surfaces has tremendous practical implications for loss prevention.

To provide theoretical support for analyses of fire and explosion risk, a comprehensive investigation of the effects of various particle sizes on ignition characteristic parameters was conducted. Key parameters, namely MITL, optimal ignition position, delay time, and self-heating rate of pulverised coal layer samples with different particle sizes, were measured using a dust layer ignition apparatus. Heat transfer and mass transfer of the pulverised coal deposits determined on the basis of the experiment results are also explored and discussed herein.

**2. Experimental***2.1. Experimental setup*

The dust layer ignition apparatus and data collection procedure for experimentation on a hot surface followed the Chinese National

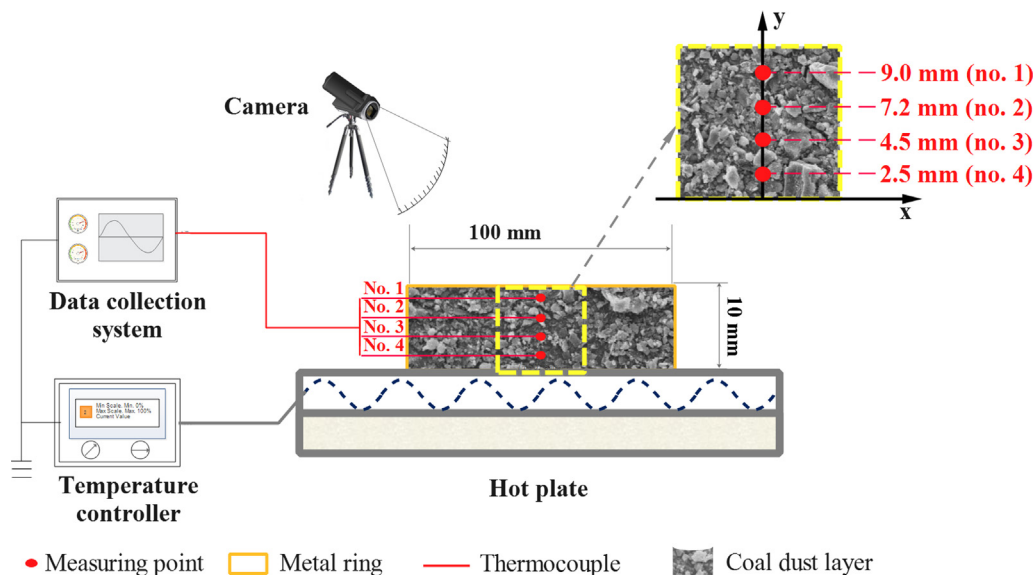


**Fig. 1.** Apparatus for investigating the ignition of coal dust deposits on a hot plate. Comparison of ignition parameters of coal samples with different sizes at a constant depth of 10 mm and constant diameter of 100 mm.

Standard, GB/T 16430-1996 [14]. The hot surface was a square aluminium plate with a dimension of  $200 \times 200 \text{ mm}^2$  and with which any desired temperature of a hot surface could be achieved within  $\pm 1 \text{ }^\circ\text{C}$ . A ring with a thickness of 4 mm, an inner diameter of 100 mm, and a height of 10 mm was placed at the centre of the plate. Then, the prepared samples with different particle sizes were gently placed inside the ring over the hot plate at the given set temperature, and the surface of the coal dust layer was smoothed out with a metal spatula [15]. This procedure was conducted carefully to ensure that the ring was completely filled with the coal dust sample. Omega K-type filament thermocouples with a diameter of 0.51 mm were selected and fixed at specific positions on the ring. Because the height of the ring was almost 20 times greater than the diameter of the thermocouple, the influence of the physical shape of the thermocouple on the structure of the tested coal dust layer was neglected in this study for simplicity. The measurement points were labelled from 1 to 4 and were positioned 9.0, 7.2, 4.5, and 2.5 mm away from the surface of the plate, respectively (see Fig. 1). The thermocouples were connected to the temperature data collector to monitor and record the coal dust layer data. The temperature of the heating plate was increased in increments of  $5 \text{ }^\circ\text{C}$  until the dust layer ignited, and at least three verification tests were performed.

The GB/T 16430-1996 standard was applied as the testing method for determining the MITL of the dust that typically poses an explosion hazard in air. The ignition of coal dust in the layer was recognised when one of the following occurred: (a) a glow, sparks, flame, or residual white ash was observed, (b) the measured temperature of the coal dust reached  $450 \text{ }^\circ\text{C}$ , or (c) the measured temperature of the dust exceeded the temperature of the furnace plate by  $250 \text{ }^\circ\text{C}$ . The coal dust was not considered to have ignited unless it was evident that an oxidation reaction had occurred and had generated a glow, flame, or combustion [16,17]. For comparison, ignition parameters of coal dust samples with different sizes were analysed at a constant sample volume.

## 2.2. Sample preparation

The coal sample used in this study was obtained from the Daliuta coal mine, Yulin City, Shaanxi Province, People's Republic of China. The sample contained 27.59% volatile compounds and 56.37% fixed carbon. This coal is widely used for gasification, power generation, and as a civil fuel. To account for the actual situation of coal dust on the mine face, the effects of the median particle size  $d_{50}$  on the self-ignition behaviour of the coal dust layer were investigated using coal dust samples with different particle sizes ( $< 80$ ,  $80\text{--}120$ , and  $120\text{--}200 \text{ }\mu\text{m}$ ). Here, these subsamples were marked as samples A, B, and C, respectively. The properties of the samples are summarised in Table 1.

Scanning electron microscopy (SEM) images of coal dust sample A were magnified 500, 1500, and 3000 times with a tungsten lamp scanning electron microscope (FEI, Model Quanta 450, USA) to observe the surface morphology, porosity, and degree of agglomeration. Moreover, the samples were subjected to particle size analysis using a Malvern Laser Particle Size Analyzer 2000 (Model Mastersizer 2000, UK).

Fig. 2 presents the particle size distribution (PSD) results of the prepared coal samples, and the characteristic diameters of the samples are listed in Table 2. The median particle size values  $d_{50}$  of samples A, B, and C were 77.86, 106.79, and 130.34  $\mu\text{m}$ , respectively. As presented in Fig. 2, the PSD of sample A ( $d_{50} = 77.86 \text{ }\mu\text{m}$ ) moved toward

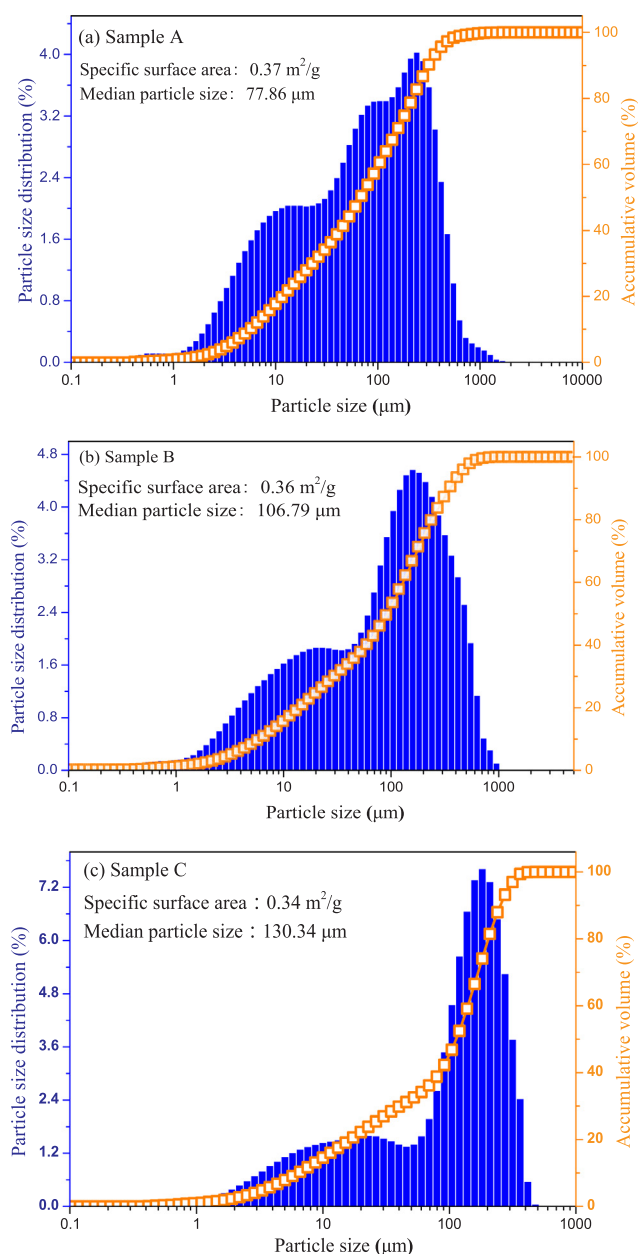


Fig. 2. Particle size analysis of the coal powder samples for (a) sample A, (b) sample B, and (c) sample C.

equilibrium, and the PSD of sample C ( $d_{50} = 130.34 \text{ }\mu\text{m}$ ) was mainly in the range of  $60.26\text{--}363.08 \text{ }\mu\text{m}$ . The specific surface sizes of samples A, B, and C were 0.37, 0.36, and  $0.34 \text{ m}^2/\text{g}$ , respectively. This revealed that specific surface area decreased as particle size increased.

Fig. 3 depicts the microstructure properties of sample A ( $d_{50} = 77.86 \text{ }\mu\text{m}$ ). The SEM images presented in Fig. 3(a) illustrate that the particle size of the pulverised coal particles was relatively uniform. More details were observed at 1500 times magnification [Fig. 3(b)]. At this magnification level, the coal particles principally appeared as long strips and polyhedrons with sharp corners, flat surfaces, and relatively

Table 1

Material properties of the coal sample.

$V_{\text{ad}}$ (%)	$M_{\text{ad}}$ (%)	$A_{\text{ad}}$ (%)	$FC_{\text{ad}}$ (%)	$C_{\text{daf}}$ (%)	$H_{\text{daf}}$ (%)	$N_{\text{daf}}$ (%)	$O^*$ (%)	$S$ (%)
27.59	10.73	5.31	56.37	71.61	4.11	0.79	7.27	0.18

Notes: ad: air-dried basis; daf: dry ash-free basis; \*Oxygen content was calculated by difference.

**Table 2**  
Characteristic diameters of coal samples A, B, and C.

Powders	$d_{90}$ ( $\mu\text{m}$ )	$d_{50}$ ( $\mu\text{m}$ )	$d_{10}$ ( $\mu\text{m}$ )	$d_{4,3}$ ( $\mu\text{m}$ )	$d_{3,2}$ ( $\mu\text{m}$ )	Average specific surface area ( $\text{m}^2/\text{g}$ )
Sample A	358.77	77.86	6.43	140.93	16.05	0.37
Sample B	406.69	106.79	7.01	160.03	16.60	0.36
Sample C	289.51	130.34	7.30	137.32	17.46	0.34

few pores. Moreover, the pulverised coal particles illustrated in Fig. 3(c) exhibited agglomeration effects. The formation of agglomerates may have been caused by van der Waals and electrostatic forces between the particles [18,19]. Finer coal particles were more able to form agglomerates because of the considerably stronger intermolecular forces involved.

### 3. Results and discussion

#### 3.1. Ignition and smouldering process of the coal dust layer

Smouldering is an essentially slow, self-sustaining type of thermal combustion with limited oxygen diffusion and flameless burning of porous fuels [20]. Fig. 4 presents the smouldering process of the coal dust deposits (samples A, B, and C) on a hot plate at 210 °C. Ignition occurred at this temperature. As presented in Fig. 4(a), several fine fissures first emerged between the metal ring and the dust layer after 15 min of heating. The sample near the metal ring experienced a higher amount of heat from the ring, which caused faster water evaporation and faster mass loss at the edge of the particle layer. Numerous cracks appeared inside the sample after approximately 30 min of heating. The development of cracks caused the entry of oxygen into the dust layer, thus resulting in the acceleration of the sample's devolatilisation rate [21]. The crack widened after approximately 45 min of heating. This widening allowed the diffusion of a higher amount of oxygen, thus increasing the intensity of the coal–oxygen composite reaction. By the end of the experiment, after 60 min of heating, a minute amount of white ash (carbonaceous char residue) was observed around the crack, thus indicating that the combustion phenomenon had occurred. No burning flame was observed during the entire experiment, but a few sparks occurred in the white ash residue. However, a considerable amount of smoke was generated during the smouldering process, and a small amount of white ash appeared in the areas around the cracks. Therefore, based on the definition of ignition used in this study, ignition occurred, because white ash residue was observed.

#### 3.2. Optimal ignition position in the coal dust layer

The position in the dust layer where the temperature first increased to the point of ignition was defined as the optimal ignition position (OIP). Fig. 5 delineates the temperature evolution of sample A on the hot plate at 200 and 210 °C. When the hot plate temperature reached 200 °C, the temperature inside the coal powder layer, as presented in

Fig. 5(a), was distinctly lower than the preset temperature of the hot plate. Self-ignition was not observed in this test. This result indicated that heat accumulation and heat loss in the coal powder layer were balanced before ignition. Moreover, for the temperature distribution of the pulverised coal bed, the temperature of the coal increased as the dust layer decreased in height. Ignition occurred in the coal dust layer when the hot plate temperature was set to 210 °C. Ignition occurred in the coal dust layer when the hot plate temperature was set to 210 °C. As evident in Fig. 5(b), the internal temperature of the dust layer exhibited a rising trend after heating treatment. Thermocouple no. 1 in the dust layer reached the first inflection point at 20.7 min, followed by the second point at 20.9 min, the third point at 22.6 min, and finally the fourth point at 23.5 min. This indicated that the coal dust at the surface of the dust layer first attained the state of thermal runaway. Joshi et al. [22] determined that ignition occurred and was accompanied by an oxidative exothermic reaction. The energy inside the coal powder layer accumulated promptly. However, heat loss occurred continuously due to heat radiation and a natural convection effect between the upper surface of the coal powder layer and the exiting air [23]. Thus, ignition did not occur at measuring point 1. The temperature at the second measuring point in the dust layer reached the highest value of 435.07 °C among the four measuring points during the combustion process. Given the combined effects of these factors, the OIP of the pulverised coal dust layer was considered to be 7.2 mm away from the hot plate (measuring point 2). The same results were obtained for samples B and C.

#### 3.3. Influence of coal particle size on ignition characteristic temperature

The MITLs of various particle sizes from the samples are illustrated in Fig. 6. The MITL of both samples A ( $d_{50} = 77.86 \mu\text{m}$ ) and B ( $d_{50} = 106.79 \mu\text{m}$ ) was in the temperature range of 200–205 °C; the MITL of sample C ( $d_{50} = 130.34 \mu\text{m}$ ) was in the range of 205–210 °C. In general, the MITL of the pulverised coal layer increased as particle size increased [12,24]; however, the effect of particle size for samples A and B on the MITL was not obvious. According to PSD and SEM results, fine particles agglomerated more easily than large particles (See Fig. 3). For coal dust particles with the same volatile content, ignition behaviour was governed by the heat transfer of the limiting geometric surface in a thermodynamic state space and by the oxygen diffusion rate. The oxygen was diffused through the micro-aisle formed by the particles' alignments. The agglomeration reduced the width of the microchannel between the particles, and oxygen took more time to arrive at the surface of particles in the cluster due to viscous resistance. Therefore,

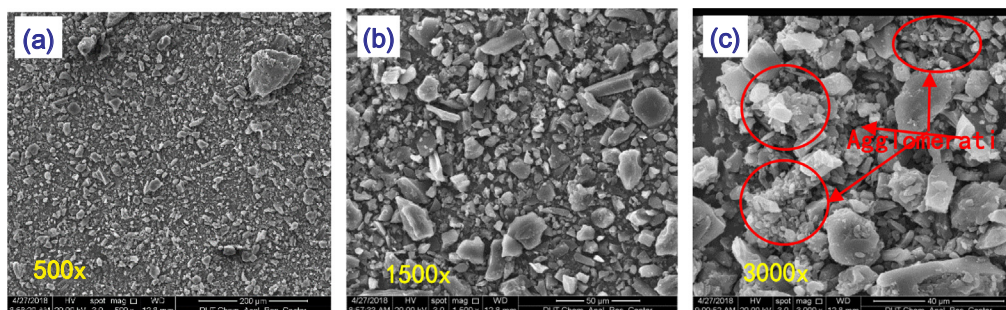


**Fig. 3.** Magnified scanning electron microscopy images of sample A ( $d_{50} = 77.86 \mu\text{m}$ ): (a) 500, (b) 1500, and (c) 3000 times.

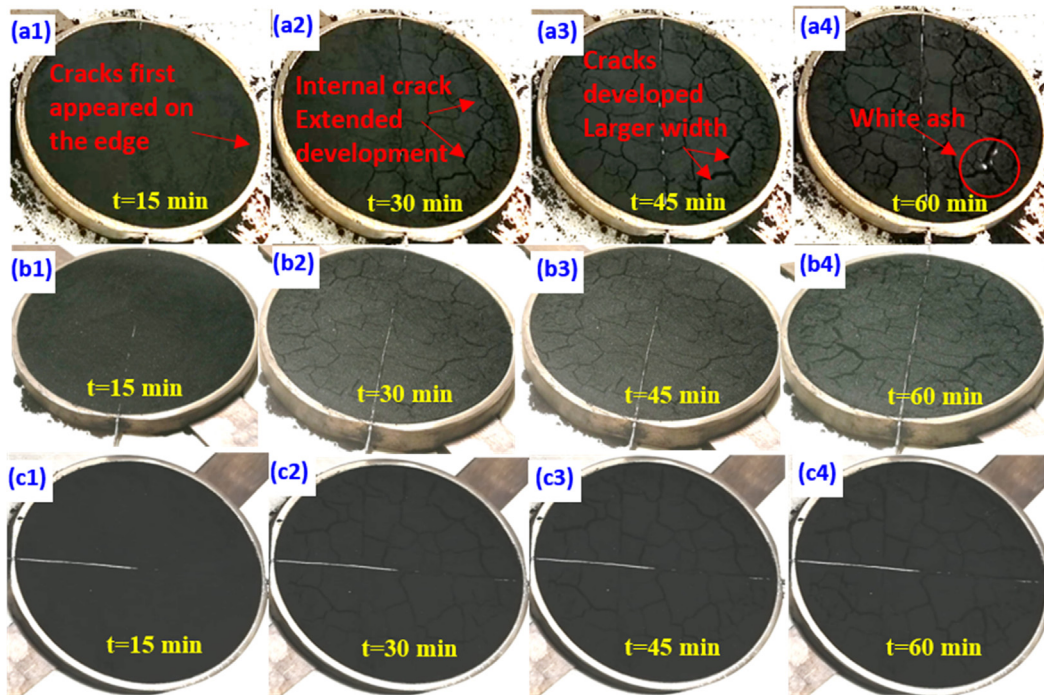


Fig. 4. Smouldering process of coal dust deposit at a hot plate temperature of 210 °C for sample A (a1–a4), sample B (b1–b4), and sample C (c1–c4).

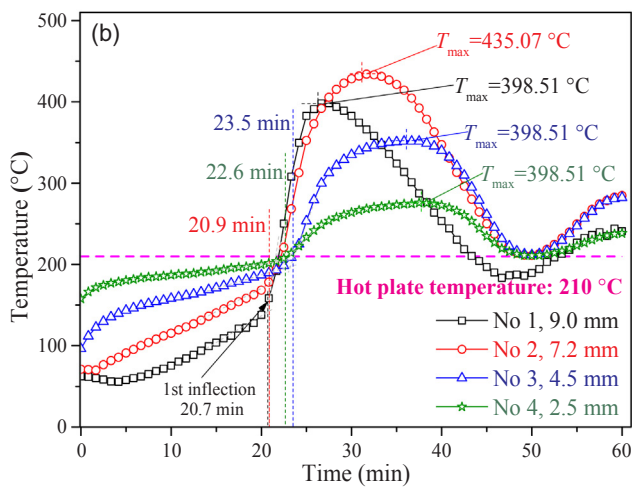
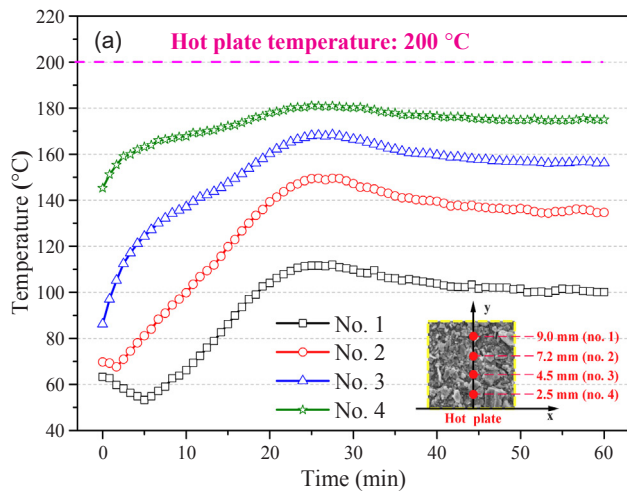


Fig. 5. Temperature history of sample A (a) with a hot plate temperature of 200 °C and (b) with a hot plate temperature of 210 °C.

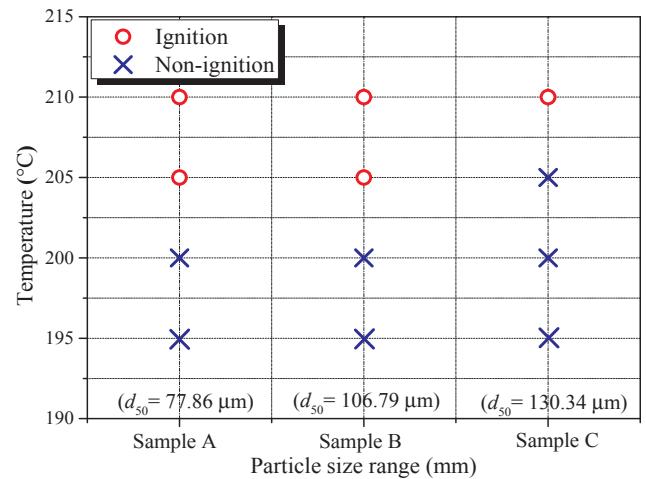


Fig. 6. MITL for coal samples with various particle sizes.

the agglomeration effects produced a higher MITL inside the sample. Fig. 7 displays the temperature evolutions of the samples with different particle sizes. As seen in Fig. 7, the highest temperatures in the layer (HTLs) of samples A, B, and C were 436.3, 427.4, and 391.3 °C, respectively. Temperature gradually decreased as the particle size increased. Oxygen transportation in a dust pile depends not only on the volume and geometry of a particle but also its size, void fraction, and specific surface area [11]. Coal powder with smaller-sized particles had a larger specific surface area (see Table 2), higher number of internal pores, and a larger contact area for oxidation reactions than coal powder with larger-sized particles [25]. The effect of increased agglomeration contributed to superior heat retention, which increased the HTL inside the sample.

### 3.4. Influence of coal particle size on ignition characteristic time

This section reports the results of the investigation of the influence of different particle sizes of pulverised coal powder on the two

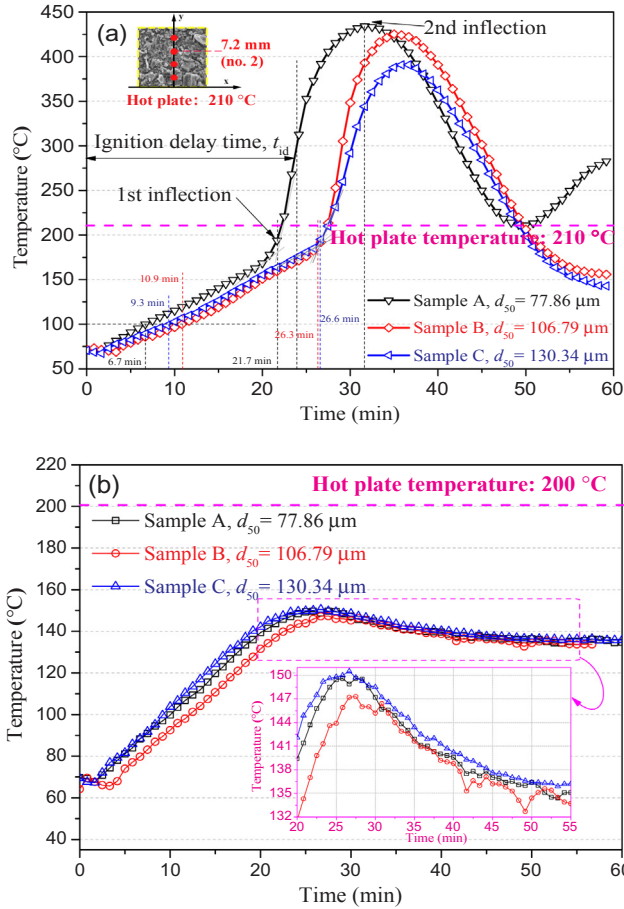


Fig. 7. Temperature evolution of the samples at 7.2 mm from the hot plate: (a) an ignition occurred when the hot plate temperature was 210 °C, and (b) no ignition was observed at a hot plate temperature of 200 °C.

characteristic time parameters—ignition delay time ( $t_{id}$ ) and time to maximum temperature ( $t_{max}$ ). Ignition delay time was defined as being from the start of heating to the midpoint of rapid temperature increase [22,25]. With respect to fire safety, detecting  $t_{id}$  is crucial for determining and controlling the thermal runaway of a coal dust layer from room temperature to the ignition stage [15]. Fig. 8 illustrates the self-heating rate versus time (min) of the pulverised coal at a depth of 7.2 mm in a layer (measuring point no. 2). The  $t_{id}$  and  $t_{max}$  of different particle sizes of the samples at measuring point no. 2 are presented in Fig. 9. Ignition occurred at 210 °C. At the beginning of the experiment (< 20 min; Fig. 8), the internal self-heating rate of the samples remained stable. Subsequently, the self-heating rate increased rapidly and reached the highest value of 37.02–57.18 °C/min after 22–32 min. Then, the value declined sharply to a negative value after 32–38 min of heating. A negative value for the self-heating rate signifies that the temperature of the coal dust layer began decreasing gradually. After 40–48 min, the self-heating rates of the different particle sizes had descended to their minimum value. The heating rate of sample A reached its peak first, followed by samples B and C. The self-heating rate of sample C peaked as the ignited layer reached 37.02 °C/min and was lower than that of the other two samples. As presented in Fig. 9, both  $t_{id}$  and  $t_{max}$  increased with the particle size of the pulverised coal. The results are consistent with the references [9,23].

### 3.5. Ideal spatial particle arrangement and geometry state

Numerous heterogeneous reactions, such as evaporation, oxidation, and pyrolysis, occurred in the self-ignition process of the samples due to

the complicated composition of coal dust and its nonuniform physical structure [26]. The particle size, volume, geometry, and porosity of the sample dominated the convective gas flow by adjusting oxygen transportation within the coal dust layers [18]. Thus, two types of arrangements in the geometry states of the samples were assumed as the means by which to observe the change in the void fraction for different particle sizes. In the model proposed in this study, the coal particles were spherical with the same diameter  $d$ , and the structure of the coal powder layer was uniform (i.e., cases 1 and 2 in Fig. 10). In the ideal spatial model designated as case 1, any particle in the upper layer was placed directly on top of another particle in the lower layer. For case 2, any particle from the upper layer was placed on top of two particles in the lower layer. The arrangement angle was between the horizontal plane of the lower layer and a line connecting the centres of the contacting particles in the upper layer. The arrangement angles  $\alpha$  for cases 1 and 2 were 90° and 60°, respectively. Due to these packing geometries, case 2 was more stable than case 1 because of a higher number of contact points between the upper and lower layers. For this reason, only the result of the case 2 arrangement is presented in the following sections.

The void fraction of the coal powder layer was defined as Eq. (1) [27]:

$$\varepsilon = \frac{V_c - V_b}{V_c} \quad (1)$$

where  $V_c = A_c \cdot h$  and  $V_b = N_b \cdot V_{bs}$  are the control volume and the particle volume, respectively, for a control volume  $V_c$  containing a sufficient number of particles;  $A_c$  is the base area of the ring,  $h$  is the height of the control volume,  $N_b$  represents the number of coal particles, and  $V_{bs}$  denotes the volume of a single coal particle,  $V_{bs} = \pi d^3/6$ .

$A_c$  and  $h$  can be expressed using Eqs. (2) and (3), respectively:

$$A_c = N_{lx} \cdot N_{ly} \cdot A = \frac{\sqrt{3}}{2} \cdot d^2 \cdot N_{lx} \cdot N_{ly} \quad (2)$$

$$h = d + (N_{lz} - 1) \cdot d \cdot \sin 60^\circ = \frac{\sqrt{3}}{2} \cdot N_{lz} \cdot d + (1 - \frac{\sqrt{3}}{2}) \cdot d \quad (3)$$

where  $N_{lx}$ ,  $N_{ly}$ , and  $N_{lz}$  are the number of particles in the  $x$ ,  $y$ , and  $z$  directions, respectively. The void fraction can be expressed using Eq. (4):

$$\varepsilon = 1 - \frac{2\pi}{9 + (6\sqrt{3} - 9) \cdot \frac{1}{N_{lz}}} \quad (4)$$

The height of the metal ring  $H$  is 10 mm, and  $d$  is equal to  $d_{50}$ . We thereby derive  $N_{lz} = 2 \cdot (H - d) / \sqrt{3} \cdot d + 1$ . Accordingly,  $N_b$  can be

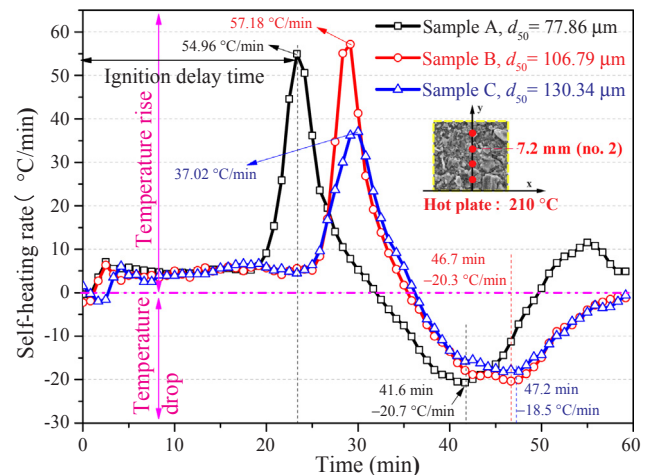


Fig. 8. Self-heating rate versus time (min) of the pulverised coal with a height of 7.2 mm in the layer.

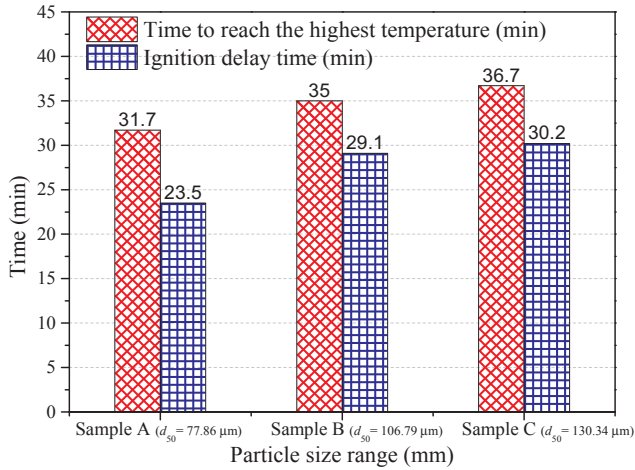


Fig. 9. Ignition delay time and time to reach the highest temperature versus the particle size range of the samples at 210 °C.

expressed using Eq. (5) [27]:

$$N_b = N_{lx} \cdot N_{ly} \cdot N_{lz} = \frac{A_c}{A} \left[ \frac{(2H-d)}{\sqrt{3} \cdot d} + 1 \right] = \frac{20000 \cdot \pi \cdot (20 - 2 \cdot d + \sqrt{3} \cdot d)}{3 \cdot d^3} \quad (5)$$

Finally, the void fraction of the coal powder layer is determined using Eq. (6):

$$\varepsilon = 1 - \frac{\frac{2}{9} \cdot \pi}{\frac{2 - \sqrt{3}}{2 \cdot (\frac{H}{d} - 1) + \sqrt{3}} + 1} \quad (6)$$

where  $H$  is fixed, as presented in Eq. (6); the void fraction  $\varepsilon$  decreases as the diameter of particle  $d$  decreases. Some geometric parameters of the coal dust deposit are listed in Table 3.

As presented in Table 3, in the case 2 arrangement, particle size had a limited effect on the void fraction for the coal dust layer in this study. Under experimental conditions, the oxygen diffusion rates were approximately equivalent for the coal dust layers due to having approximately the same void fraction across different particle sizes. However, large differences were noted in the numbers of particles for the coal samples with different particles sizes in the metal ring. In this study, devolatilisation and oxygen concentration were the main factors governing the ignition delays of the samples [28]. The oxygen reaction that first occurred in the outer surface of the coal particles and the inner surface of the pores was the dominant factor determining the temperature changes in the pulverised coal layers. The finer coal particles among all the samples had a considerably higher number of particles. Therefore, the overall specific surface areas had greater contact with oxygen, which resulted in a more intense reaction. Lower

Table 3

Geometric parameters of the dust deposit for coal samples A, B, and C.

Sample	A	B	C
$d_{50}$ ( $\mu\text{m}$ )	77.86	106.79	130.34
$N_{lx}$	148	108	88
$N_b$	886,070,862	343,281,237	188,742,794
$\varepsilon$	30.30%	30.32%	30.34%

devolatilisation of the coarser coal powder reduced the self-heating rate of the sample. The self-heating rate increased when the internal temperature increased to the point of ignition. This result explains why the finer particle size of coal dust deposits had a lower MITL and shorter  $t_{id}$ .

### 3.6. Heat transfer and mass transfer of the pulverised coal deposit

The thermochemical process in smouldering consists of the following stages: (i) drying, (ii) oxidation, (iii) ignition, and (iv) pyrolysis [29]. Different particle sizes depend on physical actions that mainly involve oxygen limitation and heat transfer (essentially through thermal generation and heat dissipation). The substantial number of combustion byproducts released as gas formation and carbonaceous layer decomposition reflect the chemical process [30]. To observe both heat and mass transfers of heterogeneous reactions, the smouldering process of pulverised coal layers with various particle sizes was divided into four stages, as shown in Fig. 11. The four stages are summarised as follows:

- (I) Coal powder layers absorbed heat from the hot plate, causing a slow increase in temperature. The finer particles in the coal samples were more readily preheated and dried on the heating plate at the same thermal condition. Moisture contained in the finer particles was more sensitive to evaporation during the heating process. The temperatures of samples A, B, and C reached 100 °C (Fig. 7) after 6.7, 9.3, and 10.8 min, respectively. A minute amount of white vapour was observed on the surface of the pulverised coal dust layer. To a certain extent, the increase in temperature resulted in the movement of oxygen molecules in the coal dust layer, and slow oxidation reactions occurred in the contact surface between the coal dust and oxygen. Several oxidation products, such as CO and CO<sub>2</sub>, were released [31]. Some fine cracks appeared in the coal powder layer, where the metal ring could be clearly observed.
- (II) The temperatures of the coal powder layer continued to increase due to heat absorption from the hot plate. The accumulation of the heat from oxidation was another cause of increase in layer temperature [32]. The oxygen absorption of coal particles and the relative devolatilisation to ignition were improved due to the preheating effect in this stage. Sample A arrived at the first inflection point after 21.7 min, sample B arrived at that point after 26.3 min, and sample C arrived at that point after 26.6 min

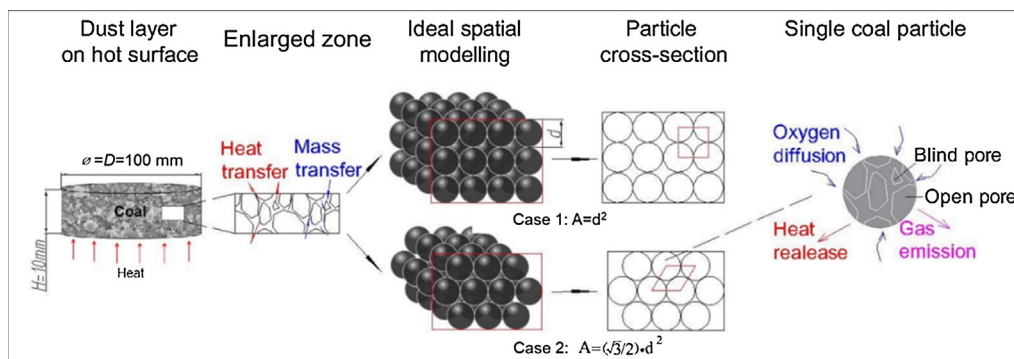


Fig. 10. Coal particles and their surface with ideal spatial modelling in a metal ring. Here,  $d$  is the diameter of a single coal particle.

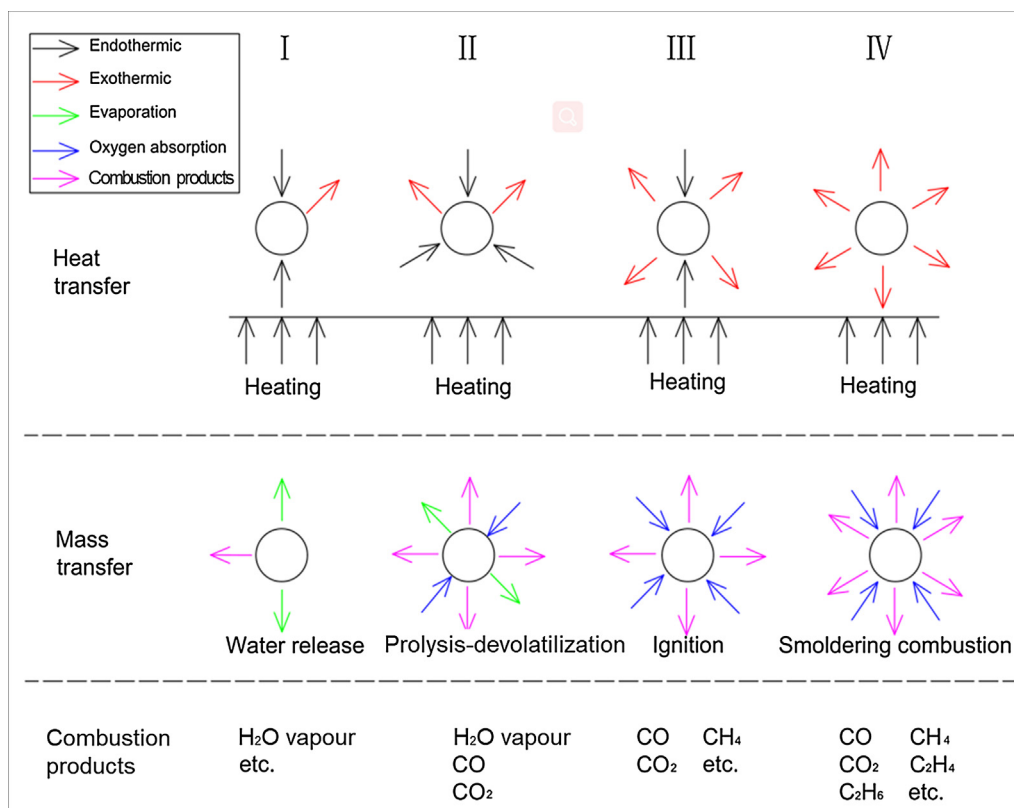


Fig. 11. Controlling the ignition mechanism of coal particles under air conditions.

(Fig. 7), which revealed that finer particles of coal dust ran out of thermal control first. The rate of coal reaction was mainly dictated by the diffusion of oxygen into the reactive centre of the particle [29]. Finer particles with larger specific surface areas (Table 2) exhibited more intensive oxidation reactions than larger particles, thus resulting in a more steady increase in gaseous products. Physical and chemical changes were consistently observed, thus leading to a further decrease in mass and volume of the sample. The volume of the pulverised coal dust decreased continuously (Fig. 4) due to the increasing oxidation rate.

(III) More cracks appeared in the interior and on the surface of the layer. The coal–oxygen reaction intensity was strongest during this stage, followed by the ignition stage. The ignition peak was first observed for a median particle size of 77.86  $\mu\text{m}$  after 31.7 min  $t_{id}$ , then observed for particles with a median size of 106.79  $\mu\text{m}$  after 35 min, and then observed for particles with a median size of 130.34  $\mu\text{m}$  after 36.7 min. The pulverised coal layer released a considerable amount of heat externally, so the temperature promptly increased to the maximum temperature of 452 °C for sample A at measuring point no. 2 [see Fig. 5(b)]. Pyrolysis reactions produced hydrocarbon gases [33]. As reported in reference [15], the volatile matter release rate of coarser particles was slower than that of finer particles due to small cohesive forces causing a wider capillary width of the coarser particles' alignment. For coal samples with finer particles, the volatile matter release rate and thermal convection were noticeably higher. For this reason, the coal with coarser particles eventually became less ignitable than the coal sample with exceptionally fine particles. Therefore, the time to ignition, time to maximum temperature, and self-heating rate were all delayed.

(IV) Sufficiently high temperatures were reached in the layer at this stage. The tarry smell of the coal dust was heavy while heating at this stage. This was because aromatic structures in the coal were destroyed under high temperature conditions, thus producing CO,

CO<sub>2</sub>, CH<sub>4</sub>, C<sub>2</sub>H<sub>4</sub>, C<sub>2</sub>H<sub>6</sub>, and phenolic compounds [34]. Mass transfer encountered high resistance, and the smouldering temperature was alleviated. Layers with finer particles sagged and collapsed more obviously. Moreover, carbonaceous char residue was distinctly apparent on the surface of sample A (Fig. 4), thus indicating that finer particle samples exhibited better combustion performance. These results were consistent with those presented in a relevant study [28].

#### 4. Conclusions

The experimental results revealed that particle size was a vital parameter for the ignition behaviour of pulverised coal deposits on a hot plate. Several hot surface tests with coal particles of different sizes were conducted to determine the MITL. The MITL for sample A ( $d_{50} = 77.86 \mu\text{m}$ ) and B ( $d_{50} = 106.79 \mu\text{m}$ ) was in the range of 200–205 °C, and the MITL for sample C ( $d_{50} = 130.34 \mu\text{m}$ ) was in the range of 205–210 °C. The agglomeration effect of fine coal particles improved the MITL of the dust layer. Moreover, the HTL of the pulverised coal layer increased as particle size decreased. As the particle size of pulverised coal increased,  $t_{id}$  and  $t_{max}$  also increased. Based on typical ideal spatial modelling, particle size had a limited effect on the void fraction but had a considerable effect on the number of particles. Moreover, the smouldering process of the pulverised coal layers with various particle sizes was divided into four stages, and the heat transfer and mass transfer processes were discussed and elucidated. The coal sample with finer particles had a substantial number of particles with a larger overall specific surface area. This specific surface area promotes greater contact between diffused oxygen and coal particles, thus resulting in a more intensive autothermal oxidation reaction. Coal dust with a smaller particle size poses a greater hazard in industrial sites, and accumulated coal dust should be removed regularly to mitigate the risk of unwanted fires and explosions.

## Acknowledgements

This work was partly supported by the National Key Research and Development Program of China (No. 2018YFC0807900), the Fundamental Research Funds for the Central Universities (No. DUT19RC(4)002), and the Open Projects of Key Laboratory of Western Mine Exploitation and Hazard Prevention, XUST (No. WME17KF01). The authors gratefully acknowledge Ms. Feinure Reheman and Ms. Yixin Wu for their experimental measurement supports.

## References

- [1] Dastidar A, Amyotte P, Going J, Chatrathi K. Inerting of coal dust explosions in laboratory- and intermediate-scale chambers. *Fuel* 2001;80(11):1593–602.
- [2] Amyotte PR. Solid inertants and their use in dust explosion prevention and mitigation. *J Loss Prev Process Ind* 2006;19(2–3):161–73.
- [3] Moron W, Ferens W, Czajka KM. Explosion of different ranks coal dust in oxy-fuel atmosphere. *Fuel Process Technol* 2016;148:388–94.
- [4] Hu ZQ, Xia Q. An integrated methodology for monitoring spontaneous combustion of coal waste dumps based on surface temperature detection. *Appl Therm Eng* 2017;122:27–38.
- [5] Sen HS, Liu ZT, Zhao EL, Lin S, Qiu LM, Qian JF, et al. Comparison of behaviour and microscopic characteristics of first and secondary explosions of coal dust. *J Loss Prev Process Ind* 2017;49:382–94.
- [6] Rice GS, Greenwald HP. Coal-dust explosibility factors indicated by experimental mine investigations 1911 to 1929. *USBM Tech Paper* 1929;464:45.
- [7] Zhang LZ, Wang X, Zhang ZQ. Numerical simulation and analysis of particle size distribution of coal dust in fully mechanized face. *Coal Mine Modern* 2017;137(2):138–41.
- [8] Chao JN, Yang HR, Wu YX, Zhang H, Lv JF, Dong WG, et al. The investigation of the coal ignition temperature and ignition characteristics in an oxygen-enriched FBR. *Fuel* 2016;183:351–8.
- [9] Hertzberg M, Cashdollar KL, NG DL, Conti RS. Domains of flammability and thermal ignitability for pulverized coals and other dusts: particle size dependences and microscopic residue analyses. *Symp (Int) Combust* 1982;19(1):1169–80.
- [10] Zhang XB, Zhao H, Yang JG. Study on the variation of coal properties for different coal diameters and its effects on combustion characteristics. *J China Coal Soc* 2011;36(06):999–1003. (in Chinese).
- [11] Polka M, Salamonowicz Z, Wolinski M, Kukfisz B. Experimental analysis of minimal ignition temperatures of a dust layer and clouds on a heated surface of selected flammable dusts. *Proc Eng* 2012;45:414–23.
- [12] Yuan CM, Huang DZ, Li C, Li G. Ignition behaviour of magnesium powder layers on a plate heated at constant temperature. *J Hazard Mater* 2013;246–247:283–90.
- [13] Garcia-Torrent J, Ramirez-Gomez A, Querol-Aragon E, Grima-Olmedo C, Medic-Pejic L. Determination of the risk of self-ignition of coals and biomass materials. *J Hazard Mater* 2012;213–214:230–5.
- [14] Dufaud O, Bideau D, Le Guyadec F, Corriou JP, Perrin L, Caleyron A. Self ignition of layers of metal powder mixtures. *Powder Technol* 2014;254:160–9.
- [15] Mohammed JA, Jafar Z, Behdad M. Experimental investigation of the minimum auto-ignition temperature (MAIT) of the coal dust layer in a hot and humid environment. *Fire Safety J* 2016;82:12–22.
- [16] Dejian W. Self-ignition characteristics of coal dusts in oxy-fuel combustion atmosphere. Leuven, Belgium: Leuven University; 2016. Doctoral dissertation.
- [17] Lebecki K, Dyduch Z, Fibich A, Sliz J. Ignition of a dust layer by a constant heat flux. *J Loss Prev Process Ind* 2003;16(4):243–8.
- [18] Yuan C, Amyotte PR, Hossain MN, Li C. Minimum ignition temperature of nano and micro Ti powder clouds in the presence of inert nano TiO<sub>2</sub> powder. *J Hazard Mater* 2014;275:1–9.
- [19] Glushkov DO, Kuznetsov GV, Strizhak PA. Experimental and numerical study of coal dust ignition by a hot particle. *Appl Therm Eng* 2018;133:774–84.
- [20] El-Sayed SA, Abdel-Latif AM. Smoldering combustion of dust layer on hot surface. *J Loss Prev Process Ind* 2000;13(6):509–17.
- [21] Huang X, Rein G. Thermochemical conversion of biomass in smoldering combustion across scales: the roles of heterogeneous kinetics, oxygen and transport phenomena. *Bioresour Technol* 2016;207:409–21.
- [22] Joshi KA, Raghavan V, Rangwala AS. An experimental study of coal dust ignition in wedge shaped hot plate configurations. *Combust Flame* 2012;159(1):376–84.
- [23] Becker A, Schiemann M, Scherer V, Shaddix C, Haxter D, Mayer J. Comparative ignition tests of coal under oxy-fuel conditions in a standardized laboratory test rig. *Fuel* 2017;208:127–36.
- [24] Mishra DP, Azam S. Experimental investigation on effects of particle size, dust concentration and dust-dispersion-air pressure on minimum ignition temperature and combustion process of coal dust clouds in a G-G furnace. *Fuel* 2018;227:424–33.
- [25] Wu DJ, Norman F, Schmidt M, Vanierschot M, Verplaetsen F, Berghmans J, et al. Numerical investigation on the self-ignition behaviour of coal dust accumulations: the roles of oxygen, diluent gas and dust volume. *Fuel* 2017;188:500–10.
- [26] Kong J, Zhao RF, Bai YH, Li GL, Zhang C, Li F. Study on the formation of phenols during coal flash pyrolysis using pyrolysis-GC/MS. *Fuel Process Technol* 2014;127:41–6.
- [27] Kim HM, Hwang CC. Heating and ignition of combustible dust layers on a hot surface: influence of layer shrinkage. *Combust Flame* 1996;105(4):471–85.
- [28] Adeosun A, Xiao ZH, Yang ZW, Yao Q, Axelbaum RL. The effects of particle size and reducing-to-oxidizing environment on coal stream ignition. *Combust Flame* 2018;195:282–91.
- [29] Miron Y, Lazzara CP. Hot-surface ignition temperatures of dust layers. *Fire Mater* 1988;12(3):115–26.
- [30] Danzi E, Marmo L, Riccio D. Minimum ignition temperature of layer and cloud dust mixtures. *J Loss Prev Process Ind* 2015;36:328–36.
- [31] Wang CP, Yang Y, Tsai YT, Deng J, Shu CM. Spontaneous combustion in six types of coal by using the simultaneous thermal analysis-Fourier transform infrared spectroscopy technique. *J Therm Anal Calorim* 2016;126(3):1591–602.
- [32] Deng J, Li B, Xiao Y, Ma L, Wang CP, Lai-wang B, et al. Combustion properties of coal gangue using thermogravimetry-Fourier transform infrared spectroscopy. *Appl Therm Eng* 2017;116:244–52.
- [33] Jayaraman K, Kok MV, Gokalp I. Thermogravimetric and mass spectrometric (TG-MS) analysis and kinetics of coal-biomass blends. *Renew Energy* 2017;101:293–300.
- [34] Luo L, Liu JX, Zhang H, Ma JF, Wang XY, Jiang XM. TG-MS-FTIR study on pyrolysis behaviour of superfine pulverized coal. *J Anal Appl Pyrol* 2017;128:64–74.